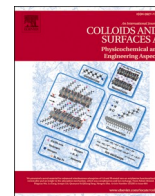




Contents lists available at ScienceDirect

# Colloids and Surfaces A: Physicochemical and Engineering Aspects

journal homepage: [www.elsevier.com/locate/colsurfa](http://www.elsevier.com/locate/colsurfa)

## Raw clays from Morocco for degradation of pollutants by Fenton-like reaction for water treatment

Ouissal Assila<sup>a,b</sup>, Zineb Bencheqroun<sup>a,c</sup>, Elisabetta Rombi<sup>d</sup>, Teresa Valente<sup>e</sup>, Amália S. Braga<sup>e</sup>, Hicham Zaitan<sup>c</sup>, Abdelhak Kherbeche<sup>b</sup>, Olívia S.G.P. Soares<sup>f,g</sup>, Manuel F.R. Pereira<sup>f,g</sup>, António M. Fonseca<sup>a,h</sup>, Pier Parpot<sup>a,h</sup>, Isabel C. Neves<sup>a,h,\*</sup>

<sup>a</sup> CQUM, Centre of Chemistry, Chemistry Department, University of Minho, Campus de Gualtar, 4710-057 Braga, Portugal

<sup>b</sup> Laboratory of Catalysis, Process, Materials and Environment, School of Technology, University Sidi Mohammed Ben Abdellah Fez, Morocco

<sup>c</sup> Processes, Materials, Environment Laboratory (LPME), Department of Chemistry, Faculty of Sciences and Technology, Sidi Mohamed Ben Abdellah University, BP. 2202, Fez, Morocco

<sup>d</sup> Dipartimento di Scienze Chimiche e Geologiche, University of Cagliari, Complesso Universitario di Monserrato, 09042 Monserrato, Italy

<sup>e</sup> ICT, Institute of Earth Sciences, Pole of the University of Minho, 4710-057 Braga, Portugal

<sup>f</sup> LSRE-LCM - Laboratory of Separation and Reaction Engineering – Laboratory of Catalysis and Materials, Faculty of Engineering, University of Porto, Portugal

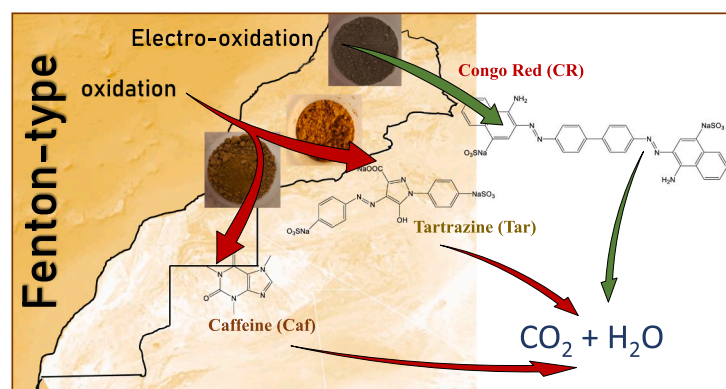
<sup>g</sup> ALiCE - Associate Laboratory in Chemical Engineering, Faculty of Engineering, University of Porto, Portugal

<sup>h</sup> CEB - Centre of Biological Engineering, University of Minho, Campus de Gualtar, 4710-057 Braga, Portugal

### HIGHLIGHTS

- Clays from Morocco as catalysts for Fenton-type oxidation of pollutants in water.
- The presence of iron at the clays surface was confirmed by XPS.
- High conversion obtained by oxidation of pollutants by Fenton-type reaction.
- Electro-Fenton-type reaction enables rapid dye mineralization at RT.

### GRAPHICAL ABSTRACT



### ARTICLE INFO

#### Keywords:

Raw clays  
Pollutants  
Water treatment  
Fenton oxidation  
Electro-Fenton  
Degradation

### ABSTRACT

Three raw clays from Morocco were used as heterogeneous catalysts for Fenton-like oxidation of organic pollutants in water. The selected pollutants were two dyes used in the textile industry, Congo Red (CR) and Tartrazine (Tar, known also as a food coloring compound, E102) and Caffeine (Caf), a stimulant drug present in popular beverages such as coffee and tea, commonly used in Morocco. Two different processes were used for their degradation: (i) Fenton-like reaction; and (ii) electro-Fenton-like reaction. Process (i) was used for Tar and Caf degradation in the presence of clays from different region of Morocco (Middle Atlas - Clay<sub>MA</sub>, Fez - Clay<sub>F</sub>, and

\* Corresponding author at: CQUM, Centre of Chemistry, Chemistry Department, University of Minho, Campus de Gualtar, 4710-057 Braga, Portugal.

E-mail address: [ineves@quimica.uminho.pt](mailto:ineves@quimica.uminho.pt) (I.C. Neves).

<https://doi.org/10.1016/j.colsurfa.2023.132630>

Received 7 July 2023; Received in revised form 4 October 2023; Accepted 19 October 2023

Available online 21 October 2023

0927-7757/© 2023 Elsevier B.V. All rights reserved.

Ourika - Clay<sub>O</sub>), the best results being obtained with Clay<sub>O</sub> and Clay<sub>MA</sub>, on which 60.0% and 23.4% of conversion and 41.0% and 20.5% of mineralization were achieved for Tar and Caf, respectively. Process (ii) was used for degrading CR by clay-modified electrodes (CME) using the rawclays from Fez and Ourika regions (Clay<sub>F</sub> and Clay<sub>O</sub>). The stability of the CME was assessed by cyclic voltammetry studies, which proved that they are stable in the experimental conditions used. The electrodegradation of CR dye, performed without hydrogen peroxide in the reaction medium, achieve 67.0% of mineralization at the end of electrolysis (2 h).

## 1. Introduction

The 2030 Agenda for Sustainable Development with its 17 sustainable development goals (SDGs) from the United Nations (UN) aims to end poverty, conserve biodiversity, combat climate change and improve the livelihoods of people everywhere [1,2]. In the 17 SDGs, water and the use of raw materials are interlinked, and chemistry and geochemistry are two of the keys to achieve these goals in order to preserve society and the planet for the future generations [3,4]. Moroccan raw clays were utilized as heterogeneous catalysts to eliminate pollutants from effluents in order to tackle the issue of clean water through the valorization of raw materials *via* the oxidation Fenton reaction. Morocco is a country with important deposits of clays and these geological materials are very attractive to apply as adsorbents [5] or heterogeneous catalysts for Fenton-like oxidation [6].

Porous materials as clays offer a word of possibilities for preparing heterogeneous catalysts due to their stability in different pH ranges, easily separation, and reutilization. Several examples can be found in the literature where clays are used as heterogeneous catalysts [7-9]. The degradation of reactive blue 19 was performed using a TiO<sub>2</sub>-coated Tunisian clay synthesized by impregnation method; it was proved that the high activity of the TiO<sub>2</sub>-coated clay in the dye degradation is due to the stability of the anatase phase in the photocatalyst [8]. A Montmorillonite clay combined with bentonite, an acid-washed clay (K10), and an Al-pillared clay ion-exchanged with nickel were used as catalysts for ethylene oligomerization in a fixed-bed continuous-flow reactor, demonstrating good activity and stability [7]. In the work of Jesus et al. [10], a natural clay was used as a support for magnetite and copper-containing magnetite in studying degradation of antibiotics

present in wastewater treatment plants effluent *via* heterogeneous Fenton/photo-Fenton reactions.

Clays are a group of minerals used as raw materials in the ceramic, paper, and metal industries, in the field of pets feeding, and as adsorbents, discoloration agents, ion exchangers, and supports [7,11-13]. These minerals are phyllosilicates with basic building blocks of Si(O, OH)<sub>4</sub> tetrahedra and M(O, OH)<sub>6</sub> octahedra, and mostly M = Al<sup>3+</sup>, Mg<sup>2+</sup> or Fe<sup>2+,3+</sup> [5,6,14].

Fenton-like oxidation reaction is very attractive, non-toxic nature, ease to use, and low cost [15-19]. However, there are few examples using clays as modified electrodes for degradation of pollutants by electro Fenton-like oxidation. Electrochemistry is one of the sustainable methods to be used for the treatment of waste effluents; indeed, it does not require high temperatures, allows the achievement of high degrees of mineralization of the pollutants, and has low operational costs [20, 21]. A further advantage comes from the possibility of carrying out the electrochemical process using electrodes modified with heterogeneous catalysts, due to their peculiar properties [22].

The work of Ozcan et al. [23] showed that iron in the kaolin clay is capable to degrade the emerging pollutant enoxacin with a TOC of 98% after 7 h of reaction. Methylene blue was also degraded with the clay-modified electrode with a chemical oxygen demand (COD) of 96.5% after 45 min of reaction [24]. Modified electrodes using iron oxide supported on nanostructured allophane clays, with both Fe<sup>3+</sup> and Fe<sup>2+</sup> species on the surface, were used for degrading atrazine with higher efficiency compared to the heterogeneous Fenton-like catalysis [25]. The clay-modified electrodes (CME) combine the advantages of the catalytic properties of the clay structures with the versatility, energy efficiency, cost effectiveness, and facility for process automation of the

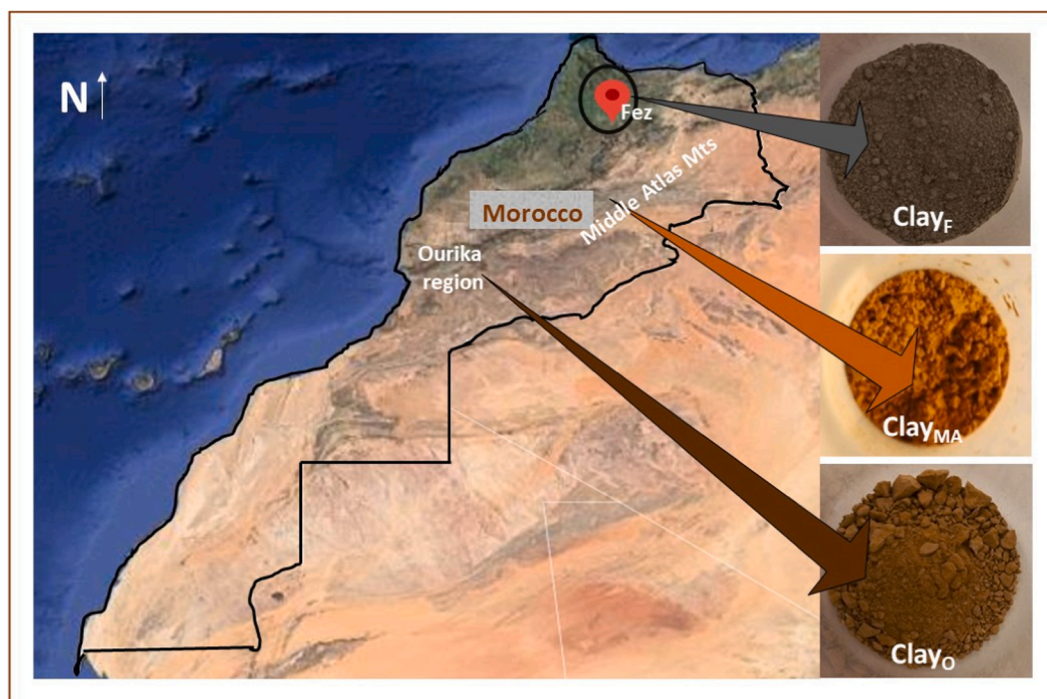


Fig. 1. Map of Morocco showing the location of the clays sites.

electrochemical processes [9].

Herein we report the degradation of different pollutants by Fenton-like reaction and electro Fenton-like oxidation using several raw clay minerals from Morocco. The places where the clays come from cover an important part of Morocco territory (Fig. 1), which confirms the presence of huge deposits of clay minerals in this country.

Two clays were collected from the Ourika region (Clay<sub>O</sub>) and the city of Fez (Clay<sub>F</sub>), while one sample was collected from the Middle Atlas region (Clay<sub>MA</sub>). They were used for studying the degradation of three different organic pollutants in water. Tartrazine (Tar) and caffeine (Caf) were removed by Fenton-like reaction using the three raw clays, whereas Congo Red (CR) was degraded by electro Fenton-like oxidation using CME based on Clay<sub>O</sub> and Clay<sub>F</sub>.

## 2. Experimental section

### 2.1. Preparation and characterization of the heterogeneous clay catalysts

Three raw clays from Morocco obtained from deposits located in the Middle Atlas region (Clay<sub>MA</sub>, where MA stands for Middle Atlas), the city of Fez (Clay<sub>F</sub>, where F stands for Fez), and the Ourika region (Clay<sub>O</sub>, where O stands for Ourika) were used in this study without any prior activation. Samples were ground, sieved to obtain particle sizes (60–100 μm), and washed with distilled water. After that, all clays were dried at 60 °C for 24 h and stored in hermetic plastic bottles until further use.

In order to study the effect of the presence of the metal in the clay, heterogeneous clay catalysts were prepared by addition of zinc or copper using an adapted method described in (Assila et al., 2023). Typically, aqueous solutions (250 mL) containing  $2.70 \times 10^{-2}$  mmol of Cu or Zn were mixed with 4 g of the pristine support (Clay<sub>MA</sub>) at pH 4.0. The suspensions were stirred during 24 h at room temperature. After each ion-exchange step, the suspensions were filtered-off, washed with deionized water, and dried at 60 °C overnight. Finally, the solids were calcined at 350 °C during 4 h under a dry-air stream. The samples were identified as Cu-Clay<sub>MA</sub> and Zn-Clay<sub>MA</sub>. All clay samples were used as heterogeneous catalysts for the degradation of tartrazine (Tar, C<sub>16</sub>H<sub>9</sub>N<sub>4</sub>Na<sub>3</sub>O<sub>9</sub>S<sub>2</sub> ≥ 90%, Sigma-Aldrich) and caffeine (Caf, C<sub>8</sub>H<sub>10</sub>N<sub>4</sub>O<sub>2</sub> ≥ 99%, Sigma-Aldrich) in Fenton-like reaction. In addition, Clay<sub>F</sub> and Clay<sub>O</sub> were used for preparing clay-modified electrodes (CME) for the degradation of Congo Red (CR, C<sub>32</sub>H<sub>22</sub>N<sub>6</sub>Na<sub>2</sub>O<sub>6</sub>S<sub>2</sub>, 3,3'-([1,1'-biphenyl]-4,4'-diyl)bis(4-aminonaphthalene-1-sulfonic acid, Sigma-Aldrich) by electro Fenton-like oxidation.

The heterogeneous clay catalysts were characterized by different techniques, such as powder X-ray diffraction (XRD), X-ray photoelectron spectroscopy (XPS), N<sub>2</sub> adsorption, scanning electron microscopy coupled with energy dispersive X-ray analysis (SEM/EDX), and chemical analysis.

Mineralogical identification was performed by XRD through a Philips X'pert Pro-MPD diffractometer (Philips PW 1710, APD), provided with an automatic divergence slit and a graphite monochromator, using CuKα radiation powdered at 40 kV and 40 mA (CuKα<sub>1</sub> = 1.54060 Å and CuKα<sub>2</sub> = 1.54443 Å). The XRD patterns were obtained from powders (bulk sample) and from oriented aggregates (< 2 μm), in the range of 2θ from 3° to 65° and from 3° to 35°, respectively, with a step size of 0.02° and a counting time of 1.25 s. Sample preparation for XRD analysis involved gentle grinding of the solid into a fine powder and packing of approximately 1.0 g of the sample into the sample holder. Identification of clay minerals was obtained in the oriented aggregates after chemical and thermal treatments (ethylene glycol saturation and heating at 490 °C).

XPS analysis was performed by recording the high-resolution and survey spectra with a Kratos Axis-Supra instrument. Monochromatic X-ray source Al Kα (1486.6 eV) was used for all samples and experiments. The residual vacuum in the X-ray analysis chamber was maintained at around  $7.2 \times 10^{-9}$  torr. The samples were fixed to the sample holder

with double sided carbon tape. Due to the non-conducting nature of the samples, it was necessary to use a co-axial electron neutralizer to minimize surface charging, which performed neutralization by itself. Charge referencing was done by setting the binding energy of C1s photo peak at 285.0 eV C 1 s hydrocarbon peak. Photoelectrons were collected from a take-off angle of 90° relative to the sample surface. The measurement was done in a Constant Analyser Energy mode (CAE) with 10 mA of emission current and 160 eV pass energy for survey spectra or 20 eV pass energy for high resolution spectra. A wide scan survey spectrum was used to identify and quantify the elements in the sample. High-resolution narrow scans were used to build the chemical state assessment, as well as to quantify the presence of the reference elements in each sample. Data analysis and atomic quantification were determined from the XPS peak areas using the ESCAPE software supplied by the manufacturer Kratos Analytical.

Nitrogen (N<sub>2</sub>) adsorption-desorption isotherms were measured at – 196 °C on an ASAP 2040 Micrometrics device. The prepared samples were previously degassed at 90 °C for 1 h and then at 250 °C with a heating rate of 5 °C min<sup>-1</sup> for 6 h, up to a residual pressure smaller than 0.5 Pa. The specific surface area and pore size distribution (PSD) were determined by the Brunauer-Emmett-Teller (BET) method and Barrett-Joyner-Halenda (BJH) analysis, respectively, using the adsorption branch.

SEM/EDX analysis was performed on a Phenom ProX with EDS detector (Phenom-World BV, Netherlands). All data were acquired using the ProSuite software integrated with the Phenom Element Identification software, allowing the quantification of the elements present in the samples, expressed in either weight or atomic percentages. The samples were added to aluminum pin stubs with electrically conductive carbon adhesive tape (PELCO Tabs™) and were imaged without coating. The aluminum pin stub was then placed inside a Phenom Charge Reduction Sample Holder (CHR), and different points were analyzed for elemental composition. EDS analysis was conducted at 15 kV with intensity map.

Chemical analysis was performed by inductively coupled plasma optical emission spectroscopy (ICP-OES) for the quantification of metals in the liquid phase during the ion-exchange process using an Optima 8000 spectrometer (PerkinElmer). A 5110 ICP-OES spectrometer (Agilent Technologies) was instead used to quantify the metals in the solid samples.

### 2.2. Fenton-like oxidation

For the degradation of Tar or Caf with the different heterogeneous clay catalysts, the concentration of pollutant (30 ppm), temperature (40 °C), and pH (=3.0) were fixed at the best values found in a preliminary study in a stirred semi-batch reactor at atmospheric pressure, using Clay<sub>MA</sub> as catalyst [6, 26]. Prior to experiments, all catalysts were pre-treated at 100 °C for 2 h in an oven. The semi-batch reactor was loaded with 250 mL of a solution of pollutant prepared with ultrapure water produced with an ultrapure water system (Milli-Q, EQ 7000), using 200 mg of catalyst and 5 mL of H<sub>2</sub>O<sub>2</sub> (12 mM). The reaction was then performed under stirring at 300 rpm, during 300 min. Sampling was carried out at fixed time intervals and the reaction was stopped with the addition of an excess of sodium sulphite (Na<sub>2</sub>SO<sub>3</sub>, Sigma-Aldrich), which instantaneously consumes the unreacted H<sub>2</sub>O<sub>2</sub>. Catalytic tests were performed in duplicate, and the maximum deviation observed in the removal of the organic pollutants was 2%. The stability of the best clay, Clay<sub>O</sub>, for Tar degradation was studied using the experimental catalytic conditions determined above. Two cycles were performed and for each cycle. The re-used catalyst was filtered-off, washed with ethanol, and dried in an oven at 70 °C overnight before reutilization. The solution recovered after each catalytic test was analyzed by ICP-OES to quantify the amount of the metal species eventually leached during reaction.

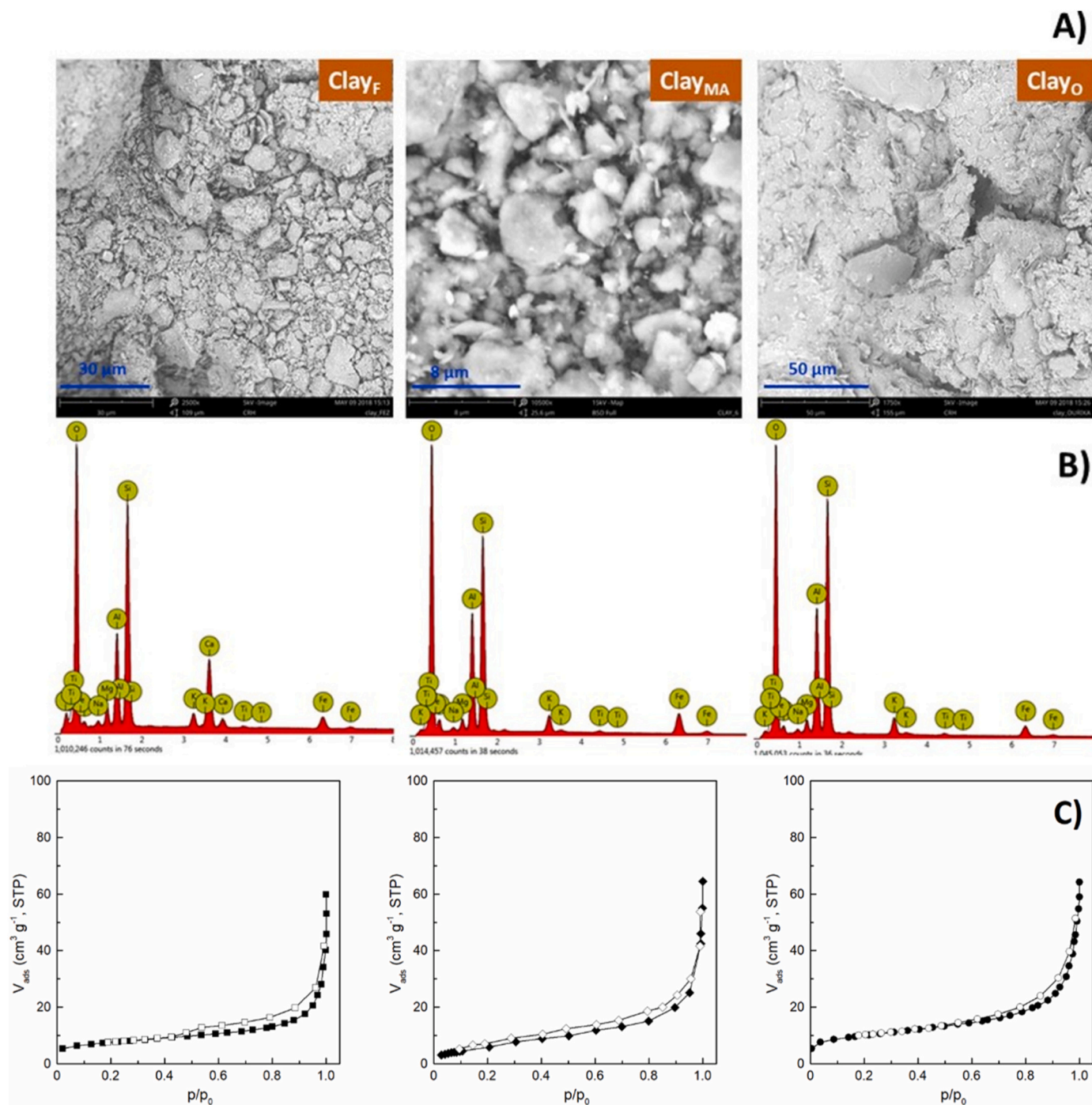


Fig. 2. A) SEM images, B) EDX spectra, and C) N<sub>2</sub>-physorption isotherms of the pristine clays.

### 2.3. Electro Fenton-like oxidation

Clay-modified electrodes (CME) were prepared using Clay<sub>F</sub> and Clay<sub>O</sub> by the procedure already described in previous papers [6,27]. Typically, CME were prepared by dispersing 20 mg of the clays powders in a mixture of 180 μL ultrapure water (Barnsted E-pure system, 18.2 MΩ cm at 20 °C) and 180 μL Nafion® suspension (5 wt%, Sigma-Aldrich). The resulting suspensions were homogenized using an ultrasound bath and totally deposited onto the wet proofed Carbon Toray paper (CT, geometrical area of 4.0 cm<sup>2</sup>, Quintech); the solvent was then evaporated at room temperature overnight. CT paper was glued to the platinum wire using a conductive carbon cement (Quintech) and subsequently dried at room temperature during 24 h.

A three-electrodes cell assembly composed of the reference electrode, consisting of a saturated calomel electrode (SCE) Hg/Hg<sub>2</sub>Cl<sub>2</sub> (KCl sat.) separated from the solution by a Haber-Luggin capillary tip, a platinum foil (99, 95%) as a counter electrode, and a CME working electrode, was used for electrochemical measurements. The electrochemical instrumentation consisted of a potentiostat/galvanostat from Amel Instruments coupled to a microcomputer (Pentium II/ 500 MHz) through an AD/DA converter. The Labview software (National Instruments) and a PCI-MIO-16E-4 I/O module were used for generating and applying the potential program as well as for acquiring data, such as current intensities.

Prior to electrochemical measurements, the solution was de-aerated with ultra-pure N<sub>2</sub> (U Quality from Air Liquide) for 30 min, and a

**Table 1**

Textural properties of the pristine clays.

Samples	$S_{\text{BET}}^{\text{a}}$ ( $\text{m}^2/\text{g}$ )	$V_{\text{total}}^{\text{b}}$ ( $\text{cm}^3/\text{g}$ )
Clay <sub>F</sub>	22.5	0.060
Clay <sub>MA</sub> [6]	23.0	0.039
Clay <sub>O</sub>	34.4	0.090

<sup>a</sup> Surface area calculated from the BET equation<sup>b</sup> Total pore volume determined from the amount adsorbed at  $p/p_0 = 0.99$ 

nitrogen stream was maintained over the solution during the measurements in order to avoid any dissolved oxygen interferences. The electrocatalytic activity of CME was investigated by using cyclic voltammetry (CV) both in the absence and in the presence of the CR dye. In the CVs, the currents were normalized with the geometrical surface area of the working electrode to provide more useful correlations in terms of kinetic issues. Electrolysis at a constant potential (2 V) in the presence of dye was carried out in the same electrolytic cell used for the CV studies. The used concentration of the CR dye was  $3.44 \times 10^{-3}$  mmol (25 ppm) for CV studies and  $6.88 \times 10^{-3}$  mmol (50 ppm) for electrolysis in 0.10 M NaCl solution, at room temperature without addition of hydrogen peroxide.

### 2.4. Product analysis

In order to quantify the extent of degradation of the organic pollutants by Fenton-like reaction, after separation of the solid catalyst by centrifugation, an UV–vis spectrophotometer (UV-2501PC from Shimadzu) was used at the characteristic wavelengths ( $\lambda_{\text{max}}$ ) of 427 nm and 272 nm for Tar and Caf, respectively, in order to determine the residual concentration of the pollutant in the reaction solution.

Liquid phase samples from electro Fenton-like reaction were analyzed by a high performance liquid chromatograph (HPLC), equipped with an isocratic pump (Jasco PU-980 Intelligent HPLC Pump) and a double on-line detection, including an UV–vis detector (Jasco Intelligent UV/vis detector). Separation of the different components was carried out using the following HPLC ion exchange columns: IonPac AS11-HC from Analytical, Aminex HPX-87 H ( $\lambda = 210$  and 260 nm) from Bio-rad, and RP18 from Merck ( $\lambda = 497$  nm).

The total organic carbon (TOC) was determined using the NPOC method, with a Shimadzu's Total Organic Carbon Analyzer TOC-L coupled with the ASI-L autosampler of the same brand.

## 3. Results and discussion

### 3.1. Characterization of the heterogeneous clay catalysts

Scanning electron microscopy (SEM) investigated the morphology of the raw clays (Fig. 2A and B), and the textural properties were evaluated by  $\text{N}_2$  adsorption analysis (Fig. 2C). SEM images obtained at different magnifications show that the clays have a heterogeneous morphology, with the presence of aggregates composed by particles of different size, with Clay<sub>MA</sub> having the smallest particles. Some of these aggregates, especially in the case of Clay<sub>O</sub>, are made up of flat intercalated layers, typical for clay minerals (Fig. 2A). From EDX spectra (Fig. 2B), the amount of the typical elements of the clays (Al, Si, Na, Mg, Fe, K, Mg, Ti, and Ca) are estimated (Table S1). The presence of high iron contents

(7.46 wt% for Clay<sub>O</sub>, 4.38 wt% for Clay<sub>F</sub>, and 5.50 wt% for Clay<sub>MA</sub>) makes these materials attractive for the Fenton reaction. Furthermore, Clay<sub>F</sub> possesses the highest calcium content (8.46 wt%), followed by Clay<sub>MA</sub> (2.40 wt%).

The  $\text{N}_2$ -physorption isotherms of Clay<sub>F</sub>, Clay<sub>MA</sub>, and Clay<sub>O</sub> are reported in Fig. 2C, and their pore size distribution (PSD) curves are shown in Fig. S1. All clays exhibit an isotherm type IIb, according to the IUPAC (International Union of Pure and Applied Chemistry) classification, with a hysteresis loop at high  $p/p_0$  values, typical for mesoporosity originating from interparticles voids [28–30]. The textural properties of the pristine clays are summarized in Table 1.

The specific surface areas calculated by the BET method are 22.5, 23.0, and 34.4  $\text{m}^2/\text{g}$  for Clay<sub>F</sub>, Clay<sub>MA</sub> [6], and Clay<sub>O</sub>, respectively. Clay<sub>O</sub> exhibits the highest values of both  $S_{\text{BET}}$  and  $V_{\text{total}}$  (1.5 times greater than those of Clay<sub>F</sub>). On the other hand, although they have similar surface areas, Clay<sub>MA</sub> has a significantly lower pore volume than Clay<sub>F</sub>.

The distribution of the pore diameters was obtained using the BJH method based on a discrete analysis of the adsorption branch of the isotherm, from which average pore diameters equal to 3.8 and smaller than 6 or 18.6 nm were estimated for Clay<sub>F</sub>, Clay<sub>O</sub> and Clay<sub>MA</sub>, respectively. These values confirm a mesoporous structure typical of the clays originated by interparticle voids, and therefore depends on the properties of the formed aggregates, which in turn depend on the properties of the particles that compose them. However, the presence of particles with a broad size distribution could lead to the formation of an irregular mesoporous structure, with a broad pore size distribution, which in turn influences the surface area values. Moreover, the particular layered structure of clays should be considered. The assembly of clay platelets into successive structures (tactoids and aggregates) is affected by the clay mineral properties, in terms of platelet-platelet bonding energy, size, packing order, and alignment, leading to more or less rigid aggregates, also characterized by a different order degree [5,31,32].

Clay<sub>MA</sub> was modified by introduction of copper or zinc in order to enhance the catalytic behavior of the pristine clay. The composition of all clays was determined by ICP-OES analysis, with Si, Al, and Fe as the most important elements. Ca, K, Ti, and Mg, typical elements of clay materials as well, were also quantified (Table 2).

Clay<sub>MA</sub> and Clay<sub>O</sub> contain higher amounts of Fe (5.40 and 6.45 wt%, respectively), whereas Clay<sub>F</sub> is richer in calcium (11.44 wt%), in agreement with EDX analysis. These differences in composition justify the different colours of the clays (Fig. 1). The presence of iron in the pristine clays is expected to enhance the catalytic properties of these materials for Fenton reactions. Furthermore, the presence of various metals such as copper (Cu), magnesium (Mg), zinc (Zn), and calcium (Ca) in the clays, along with iron, can induce the formation of hydroxyl radicals ( $\cdot\text{OH}$ ) through the activation of hydrogen peroxide ( $\text{H}_2\text{O}_2$ ), persulfate, and peroxymonosulfate. These reactions are known as Fenton-like processes.

In the case of Clay<sub>MA</sub>, the introduction of Cu or Zn leads to a remarkable decrease in the Ca and Mg contents (about 90% and 70%, respectively); a more limited variation is instead observed for K, Fe, and Ti, whose contents decrease by about 20%, 30%, and 15%, respectively. The decrease in the content of the metals present in the original clay, especially observed for Ca and Mg, is reasonably due to an ion exchange process involving such cations and those contained in the aqueous

**Table 2**ICP-OES results (wt% of metals) of the pristine clays and the two metal-containing Clay<sub>MA</sub> samples.

Sample	Si (wt%)	Al (wt%)	Na (wt%)	K (wt%)	Mg (wt%)	Ca (wt%)	Fe (wt%)	Cu (wt%)	Zn (wt%)	Ti (wt%)
Clay <sub>MA</sub>	27.06	12.05	0.25	3.68	1.86	3.69	5.40	-	-	0.51
Cu-Clay <sub>MA</sub>	27.60	11.35	0.28	2.61	0.58	0.23	4.55	0.43	-	0.43
Zn-Clay <sub>MA</sub>	27.39	11.31	0.31	2.87	0.63	0.33	4.33	-	0.32	0.46
Clay <sub>F</sub>	23.88	5.93	0.62	1.47	1.72	11.44	3.98	-	0.35	0.29
Clay <sub>O</sub>	26.43	9.89	0.31	2.52	0.96	0.35	6.45	-	-	0.50

**Table 3**

Binding energies (BE) and the amount of the elements (wt%) obtained from the XPS spectra in the C 1 s, O 1 s, Cl 2p, N 1 s and Ag 3d regions of the samples.

Sample	Clay <sub>O</sub>		Clay <sub>F</sub>		Clay <sub>MA</sub>	
	BE (eV)	wt (%)	BE (eV)	wt (%)	BE (eV)	wt (%)
Si 2p	102.56	24.71	102.96	27.24	102.73	23.75
Al 2s	119.26	9.24	119.46	7.42	119.53	10.04
O 1s	531.76	50.59	532.06	51.33	532.03	49.96
C 1s	285.06	5.30	285.06	6.77	285.13	6.60
Fe 2p <sub>1/2</sub>	724.36	1.96	725.76	1.72	725.83	1.37
Fe 2p <sub>3/2</sub>	711.76	1.99	712.66	1.33	711.93	1.76
Fe 3p	56.14	2.03	56.25	1.01	55.91	1.58

solution of the Cu or Zn precursor nitrates (*i.e.*, Cu<sup>2+</sup> or Zn<sup>2+</sup>, and H<sup>+</sup>).

All these samples were analyzed by XPS to determine the composition, the relative distribution, and the oxidation state of the components present on the surface. In agreement with ICP-OES analysis, the predominant elements in all the recorded survey XPS spectra are oxygen (O 1 s), carbon (C 1 s), iron (Fe 2p), silicon (Si 2p), and aluminum (Al 2 s), typical for clay minerals [33]. In addition, small amounts of potassium (K 2p), calcium (Ca 2p), and sodium (Na 1 s) were also detected. The binding energies (BE) of the principal elements as well as their surface amounts (wt%) are reported in Table 3.

It can be noted that the BE values are similar for all the elements irrespective of the pristine clay. By converse, some differences exist between the clays in the surface concentration of the different components, which are linked to the geological deposits where these materials came from. In particular, the surface amount of iron is in the order Clay<sub>O</sub> (5.98 wt%) > Clay<sub>MA</sub> (4.71 wt%) > Clay<sub>F</sub> (4.06%). The comparison with the chemical analysis results (Table 2) shows similar Fe contents both on the surface and in the bulk, indicating that it is homogeneously distributed throughout the clays particles.

The energy separation ( $\Delta E$ ) between the two peaks of Fe 2p is 12.6, 13.1, and 13.9 eV, for Clay<sub>O</sub>, Clay<sub>F</sub>, and Clay<sub>MA</sub>, respectively, and the presence of the Fe 3p peak suggests the existence of iron in different oxidation states. For all clay samples, the high-resolution XPS spectra

recorded in the Fe region show that both the 2p<sub>1/2</sub> and 2p<sub>3/2</sub> peaks visible in the corresponding survey spectra can be deconvoluted in three and four components, respectively (Fig. 3).

For all the samples, the Fe 2p<sub>1/2</sub> peak appears to be composed by three components at 728.7, 725.7, and 723.4 eV, whereas the Fe 2p<sub>3/2</sub> peak results from the overlapping of four contributions at BE values of 710.2, 712.6, 715.3, and 715.4 eV. These values are related to the presence of Fe<sup>3+</sup> and Fe<sup>2+</sup> in the form of oxides in the clay minerals [33-35].

The C 1 s peak at about 285 eV is ascribable to surface-atmosphere interactions or to residual precursors [36,37], whereas the O 1 s peak close to 532 eV is due to the elemental oxygen, oxides, oxygen in water, and metal oxides associated with the elements [36]. Signals of Si 2p at 103 eV and Al 2s at 119.5 eV are attributed to Si-O-Si and Si-O-Al chemical bonds, or to both atoms coordinated with other elements, typical for these type of materials [33,38]. Both the Si 2p and Al 2s peaks can be deconvoluted in three components, as shown in their high-resolution XPS spectra (Fig. S2).

For Si 2p, the presence of these three contribution in all clays suggests that Si atoms are tetrahedrally coordinated with oxygen by Si-O-Si and Si-O-Al, which confirms the presence of such bonds in these materials [33]. In addition to those of Al 2s, Al 2p peaks were identified at about 74 eV for all the pristine clays. The presence of the three components for the Al 2s signal and the appearance of the Al 2p peak close to 74 eV suggest the existence of the same coordination than for Si and the presence of Al-OH bonds where aluminum is in tetrahedral and octahedral coordination. From the literature, the binding energy values of Al 2p in the simultaneous presence of tetrahedral and octahedral Al atoms are intermediate between the binding energy values of octahedrally and tetrahedrally coordinated species [33]. Thus, the BE values at 74.14, 73.25, and 74.91 eV for Clay<sub>O</sub>, Clay<sub>F</sub>, and Clay<sub>MA</sub>, respectively, suggest that Al atoms at the clays surface have tetrahedral or/and octahedral coordination (Fig. S2).

Samples obtained by modifying Clay<sub>MA</sub> with Cu or Zn were also analyzed by XPS. Concerning the major components, their XPS profiles were similar to that of the pristine clay. The BE regions of Cu 2p and Zn 2p were also investigated to have information about the nature and the

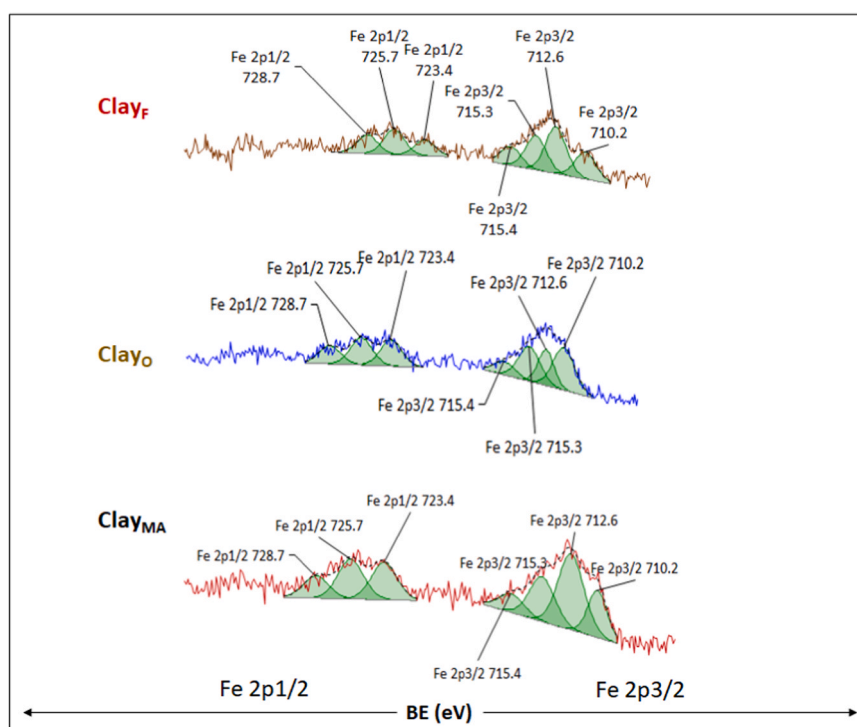


**Fig. 3.** High-resolution XPS spectra of Fe 2p of all pristine clays.

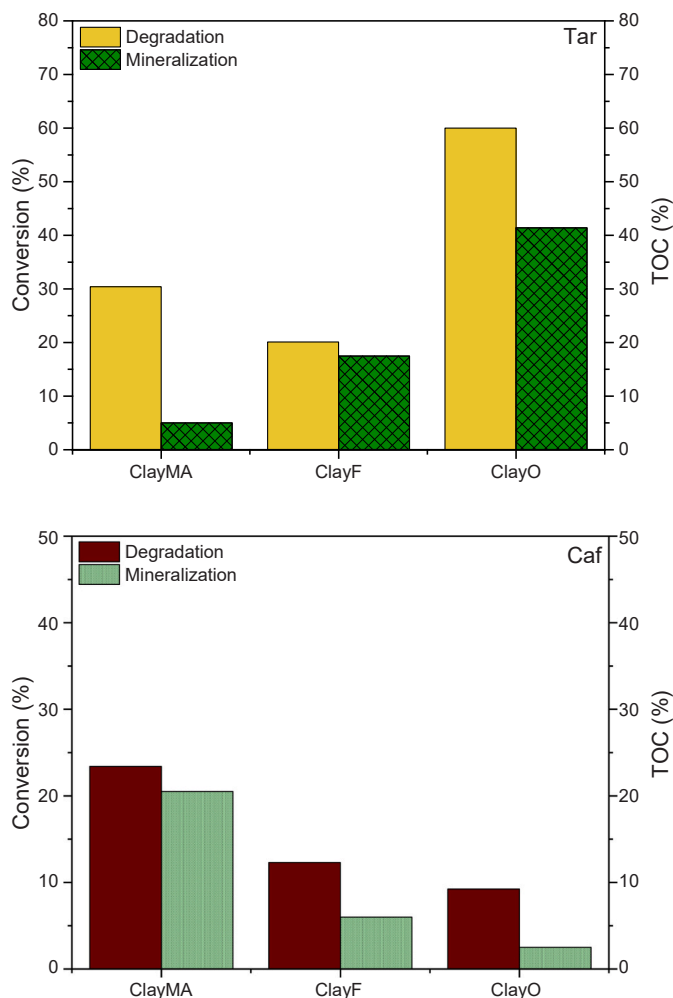


**Fig. 4.** Conversion and TOC percentages after Tar and Caf degradation by Fenton-like reaction in the presence of Clay<sub>MA</sub>, Clay<sub>F</sub>, and Clay<sub>O</sub>. Reaction conditions: 250 mL of dye solution (30 ppm); 5 mL of H<sub>2</sub>O<sub>2</sub> solution (90 mM); T = 40 °C; pH = 3.0; 0.2 g of catalyst.

surface concentration of the metals. Peaks of Cu 2p<sub>1/2</sub> and Cu 2p<sub>3/2</sub> were detected at 953.48 eV and 931.98 eV, respectively, from which a Cu surface amount of 0.47 wt% was calculated. Likewise, in the XPS spectrum of Zn-Clay<sub>MA</sub>, two peaks ascribable to Zn 2p<sub>1/2</sub> and Zn 2p<sub>3/2</sub>, respectively, were identified at 1041.11 eV and 1025.21 eV, which allowed of determining a Zn surface content of 0.34 wt%. Noteworthy, both the Cu and Zn concentrations at the surface are similar to those determined by ICP-OES analysis in the bulk (Table 2), which suggests a homogeneous distribution of the metals throughout the Clay<sub>MA</sub> particles.

The XRD pattern of the raw clay from Fez (Clay<sub>F</sub>) is presented to exemplify the identification of the detrital and clay minerals present in these materials (Fig. S3). This sample also contains non-clay minerals, typically detrital minerals like quartz, mica, and plagioclase (< 2 μm). However, the presence of reflections at 3.86, 3.04, and 2.50 θ even in the clay size fraction < 2 μm (oriented aggregates) indicates that calcite is the most abundant non-clay mineral. Illite is indicated by the 2θ values of 10.1° for d<sub>001</sub> and of 5.02° for d<sub>002</sub>, which are not influenced by EG-solvated conditions. Kaolin mineral, probably kaolinite, was identified by the d<sub>001</sub> and d<sub>002</sub> reflections at 7.06 and 3.59 2θ, respectively. Moreover, chlorite is detected by the 00 l reflections around 7.00, 4.74, and 3.55° [32]. Regarding smectite, it was identified combining the patterns of air-dried samples with those of the glycolated and heated ones. Thus, the broad reflection in the region of low 2θ, at 15.87° for the

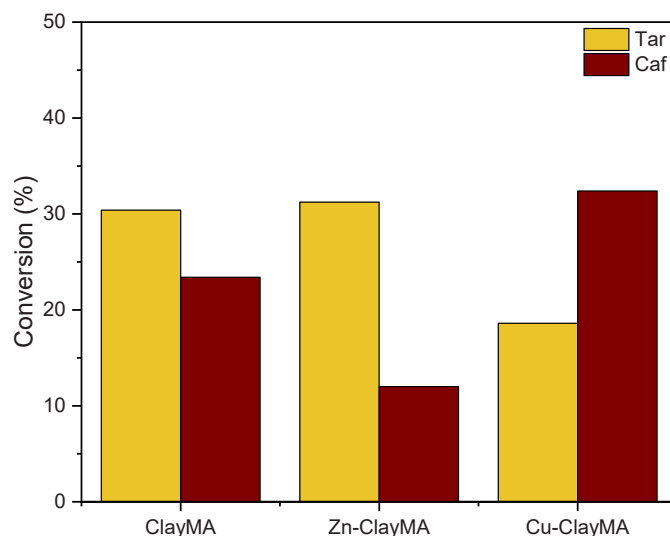


**Fig. 5.** Conversion of Tar and Caf by Fenton-like reaction in the presence of Clay<sub>MA</sub>, Zn-Clay<sub>MA</sub>, and Cu-Clay<sub>MA</sub>. Reaction conditions: 250 mL of dye solution (30 ppm); 5 mL of H<sub>2</sub>O<sub>2</sub> solution (90 mM); T = 40 °C; pH = 3.0; 0.2 g of catalyst.

air-dried sample, is expanded to approximately 17° for the EG-solvated. After heating, this peak collapses to 10 2θ, which is characteristic of the smectite mineral phase. Iron oxyhydroxide goethite is present in trace amounts, as indicated by a weak, but typical reflection at 2θ values of 2.69–2.70°. As Clay<sub>F</sub>, Clay<sub>O</sub> also contains illite and kaolin mineral, but the other phases are interstratified vermiculite-chlorite and goethite.

### 3.2. Fenton-like reaction of the dyes

The choice of the oxidation reaction is reliant on the nature of the pollutants and their stability in Fenton-like reaction. The Fenton reaction is distinguished by the combination of ferrous salts and hydrogen peroxide, culminating in the generation of hydroxyl radicals (•OH) that swiftly drive the decomposition of pollutants [6,16,19,26]. Notably, clays contain a significant iron content, which plays a crucial role in promoting degradation through the Fenton process. Furthermore, they also contain other cations that can facilitate the reaction (Table 2).

Concerning the pollutants, they were chosen due their presence in aqueous effluents in Morocco. Congo Red (CR) and Tartrazine (Tar) are azo molecules, di and mono, respectively, while caffeine (Caf) is a purine molecule based in an xanthine core with two fused rings, a pyrimidinedione and imidazole, in which the three methyl groups are located at positions 1, 3, and 7 (Fig. S4). Azo molecules are more easily oxidized than the purine molecules by Fenton reaction [6,16,19,26].

Tar and Caf were studied by a typical Fenton-like reaction with all the pristine clays. Moreover, in order to improve the efficacy of the degradation of these pollutants, two new heterogeneous catalysts were prepared from Clay<sub>MA</sub> by the introduction of copper (Cu-Clay<sub>MA</sub>) or zinc (Zn-Clay<sub>MA</sub>).

The catalytic results obtained with the different heterogeneous catalysts for the degradation of Tar and Caf through Fenton-like reaction, using the experimental conditions determined in [4], are displayed in Figs. 4 and 5. Blank runs were also made in the presence of only hydrogen peroxide or raw clays. Hydrogen peroxide by itself was unable to degrade the dyes; indeed, only 4% of conversion was determined after 5 h of reaction. Similarly, the adsorption tests showed that the clays were able to remove less than 3% of the dyes after 5 h of reaction. These results suggest that the simultaneous presence of H<sub>2</sub>O<sub>2</sub> and clays is required to successfully remove dyes from aqueous media through the Fenton-like reaction.

Fig. 4 displays the results for Tar and Caf degradation in terms of

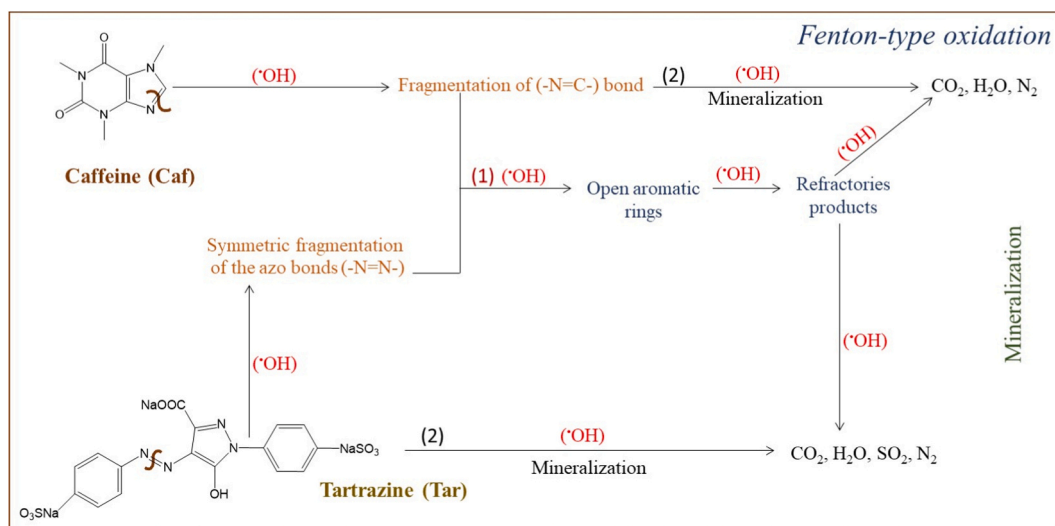


Fig. 6. Proposed mechanism pathways for Fenton-like degradation of Caf and Tar molecules.

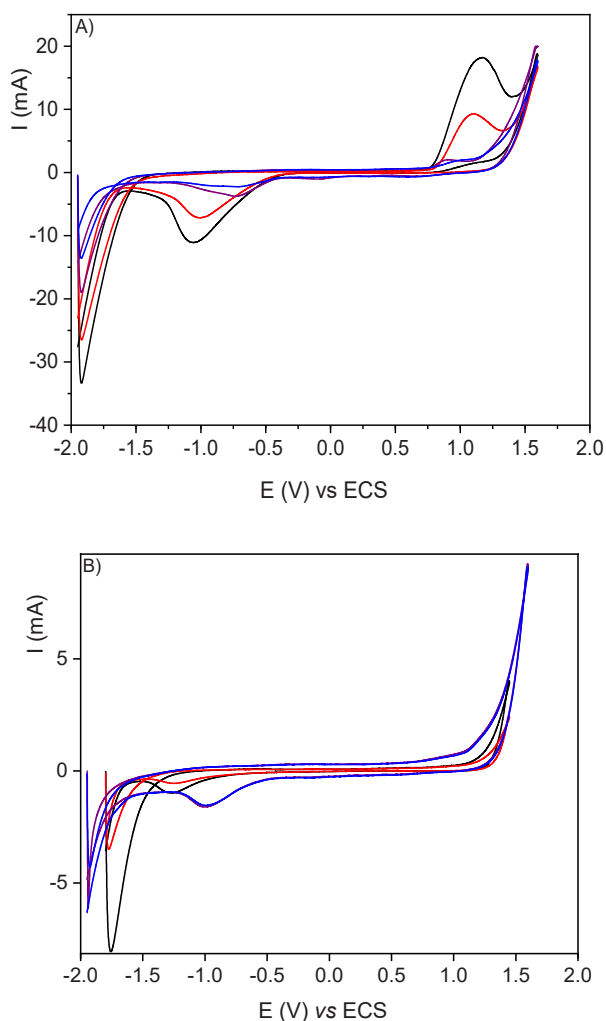


Fig. 7. Cyclic voltammograms of the CME based on: A) Clay<sub>F</sub> and B) Clay<sub>O</sub> at a scan rate of 50 mVs<sup>-1</sup>, in the absence of dye (black and red curves) and in the presence of 25 ppm of CR (blue and violet curves) in NaCl (0.10 M).

both pollutant's conversion and TOC, after 5 h of reaction in the presence of the clay catalysts.

All clays are more effective in degrading Tar than Caf, with Clay<sub>O</sub> showing the best performance, achieving in the case of Tar 60% of conversion and 41.5% of mineralization. This suggests that the catalyst can favor the formation of hydroxyl (\*OH) radicals responsible for Tar degradation. On the other hand, Clay<sub>MA</sub> and Clay<sub>F</sub> show a much lower removal capacity, reaching conversion values of 30.5% and 20.1%, respectively. Notably, although the conversion is higher for Clay<sub>MA</sub>, the degree of mineralization for this catalyst is only 5%.

In the case of Caf degradation, the behavior of the clay catalysts is different, with Clay<sub>MA</sub> being the best one with 23.4% of conversion. The low values obtained for Caf conversion in the presence of the raw clays confirm that the caffeine molecule is very stable, and the catalysts are not able to fully convert the pollutant initially present (30 ppm), despite the good mineralization degree for Clay<sub>MA</sub> (20.5%), followed by the considerably lower ones for Clay<sub>F</sub> (6%) and Clay<sub>O</sub> (2.5%). These catalytic results are not only dependent on the molecular structure of the pollutants but also on the chemical composition and the geological place of the clays. For Tar degradation, a clay rich in iron at the surface (Clay<sub>O</sub>, Fe = 5.98 wt%) enhances the Fenton-like reaction, followed by Clay<sub>F</sub>, which has a lower iron content but a higher amount of calcium (Tables 2 and 3).

To investigate the effect of Zn or Cu addition on the catalytic behavior of Clay<sub>MA</sub>, the Fenton-like reaction was studied using both Zn-Clay<sub>MA</sub> and Cu-Clay<sub>MA</sub> as heterogeneous catalysts for the removal of both dyes. The pertinent results are compared with those obtained for the pristine clay in Fig. 5.

Zn-Clay<sub>MA</sub> and Clay<sub>MA</sub> have the same behavior for Tar conversion, which suggests that the presence of Zn does not improve its degradation. In addition, the presence of copper leads to worst performance. By converse, for Caf degradation the presence of copper improves the oxidation of the molecule (32.4%) compared to the pristine clay, whereas the presence of Zn is detrimental for the catalyst, which loses its activity.

From the catalytic results obtained for the Fenton-like reaction, the best catalysts turned out to be the raw clay from Ourika region (Clay<sub>O</sub>) and the Cu-Clay<sub>MA</sub> sample for Tar and Caf degradation, respectively.

The stability of Clay<sub>O</sub> in the Fenton-like oxidation of Tar was studied by performing two reaction-regeneration cycles, and the same catalytic behavior was observed. In addition, after each reaction test, the amount of leached metals was measured by ICP-OES and no dissolution was detected (within the experimental error) in all the experiments, indicating that the catalysts are stable under the experimental conditions



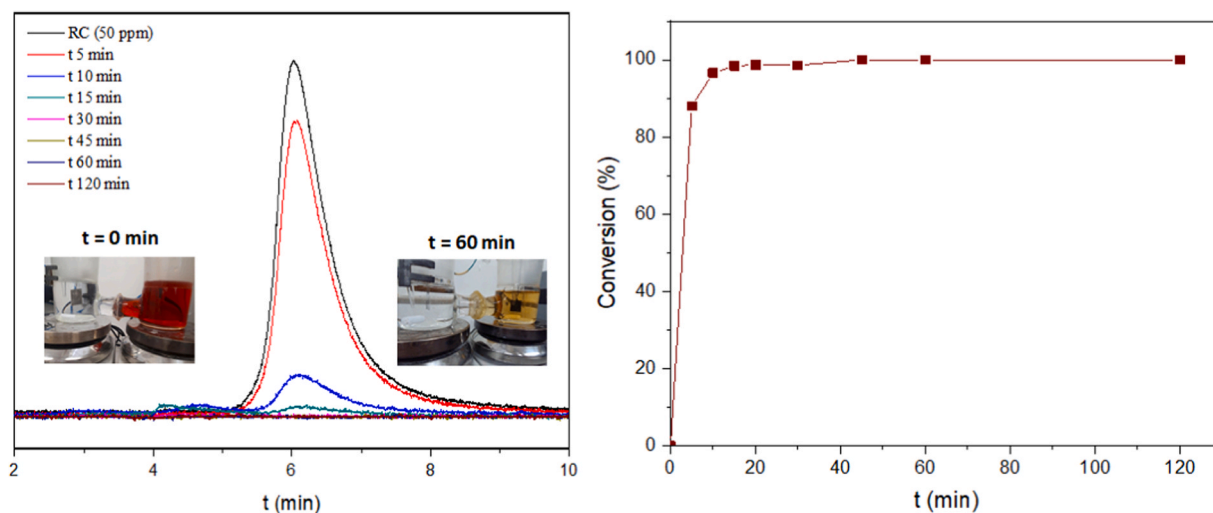


Fig. 8. HPLC-UV/vis chromatograms and the conversion of CR (■) vs. electrolysis time for the electrooxidation of CR in the presence of Clay<sub>F</sub>-modified electrode.

used.

Fenton reaction occurs between iron and H<sub>2</sub>O<sub>2</sub> to generate highly oxidative hydroxyl radicals (<sup>•</sup>OH), which are efficient in degrading pollutants in water. However, in the heterogeneous Fenton reaction, Fe is stabilized within the material's structure and generates <sup>•</sup>OH without the precipitation of iron hydroxide. The presence of iron at the clays surface allows enhancing the heterogeneous Fenton catalysis. In addition, other metals as Cu, Mg, Zn, or Ca, identified in the clays, together with iron can trigger not only H<sub>2</sub>O<sub>2</sub> but also persulfate and peroxy-monosulfate to generate <sup>•</sup>OH, the latter of which are known as Fenton-like reactions [39,40]. Both pollutants are degraded by the attack of the hydroxyl radicals (<sup>•</sup>OH) produced during the Fenton-like reaction. The following catalytic degradation pathways of Tar and Caf in the presence of clays by Fenton-like reaction can be proposed (Fig. 6).

Decomposition of the Tar molecule follows a symmetric degradation of the -N = N- azo bond, since in the UV/vis spectrum, the band assigned at 260 nm disappears after 45 min of reaction and the band at 427 nm decreases in intensity (Assila et al., 2023b). In the case of Caf, which is a stable molecule, degradation could occur through the attack on the -N = C- bond in the aromatic rings of the purine structure (Assila et al., 2023a). For both pollutants, after the attack of the first radical, the total opening of the aromatic rings occurs, passing through the formation of low molecular weight organic acids (refractory products) and finally reaching mineralization (pathway 1). The direct mineralization of the pollutants seems to be more difficult, due to the presence of the refractory products (pathway 2).

Being not stable in the acidic medium used in the Fenton-like reaction because of its precipitation, the Congo red (CR) dye degradation was instead performed through the electro Fenton-like reaction, using Clay<sub>F</sub>- and Clay<sub>O</sub>-modified electrodes. In our previous work, CR was degraded using Fe-zeolite modified catalysts based on different zeolite structures [41]. In that case, the Fe-(H)ZSM-5 modified catalysts showed the best degradation results due to the acidic properties of the MFI structure [41].

The cyclic voltammometry studies between -2.0 V and +2.0 V vs. SCE potential with the clay-modified electrodes based on Clay<sub>O</sub> and Clay<sub>F</sub> on Carbon Toray (CT) were performed with a scan rate of 50 mVs<sup>-1</sup> in the presence of NaCl as the electrolyte or with the CR dye (25 ppm), at room temperature (Fig. 7).

The electro behavior of the CME are different and it is probably related to the presence of different iron species, i.e. the Fe(II)/Fe(III) couple, or other cations present on the surface of both clays, as determined by ICP-OES and XPS analyses (Tables 2 and 3). The Clay<sub>O</sub>-modified electrode in the absence of CR dye (black and red curves)

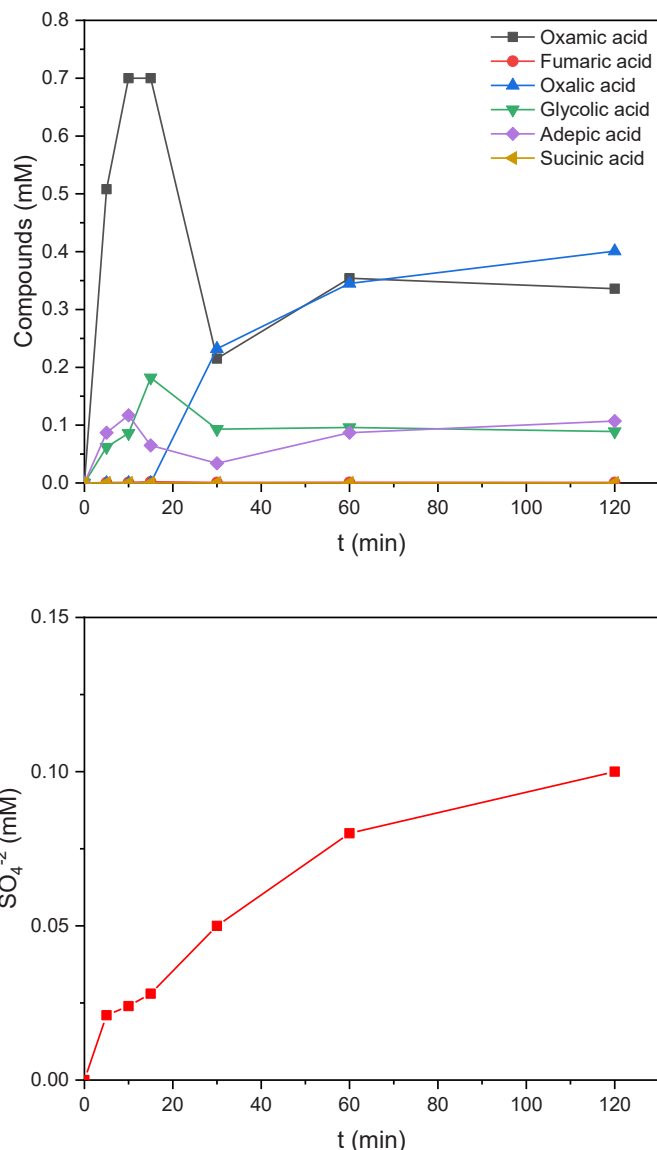
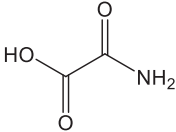
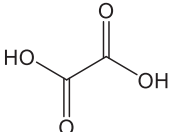
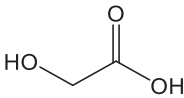
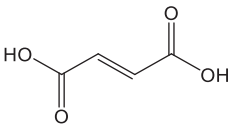
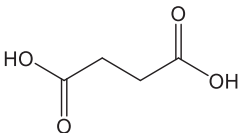
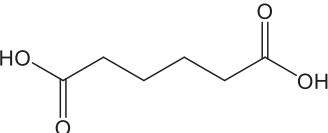


Fig. 9. The evolution of the compounds and sulfate ions during the electrolysis of CR in presence of CME based in Clay<sub>F</sub>.

**Table 4**  
Identification of the byproducts.

Byproduct	Concentration (mM)	Percentage (%)
Oxamic acid 	0.336	36
Oxalic acid 	0.401	43
Glycolic acid 	0.089	9.5
Fumaric acid 	0.011	< 0.1
Succinic acid 	$0.5 \times 10^{-5}$	< 0.01
Adepic acid 	0.117	11.5

shows one irreversible cathodic process at  $-1.3$  V vs. SCE in 0.1 M NaCl medium. For the raw clay from Fez City, an anodic redox process is observed at 1.2 V vs. SCE, and in the reverse scan of the potential a reduction peak can be seen at  $-1.0$  V vs. SCE.

In the presence of CR dye (blue and violet curves), both CME are active and show an increment in the anodic process, attributed to the catalytic activity of the catalysts. The oxidation of CR starts at 0.8 V and 1.1 V vs. SCE for Clay<sub>F</sub> and Clay<sub>O</sub>, respectively, after the oxidation of Fe(II) into Fe(III), indicating that the presence of Fe(III) species on the electrode surface is necessary for the oxidation of this organic dye [41].

The rate-determining step of the CR oxidation process can be determined by voltammetry studies, where the slope of the  $\log I$  (mA) vs.  $v$  ( $\text{mVs}^{-1}$ ) curves in 0.1 M NaCl medium corresponds to 0.62 and 0.55 for Clay<sub>F</sub> and Clay<sub>O</sub>, respectively. These values are consistent with a kinetics of the electrochemical reaction governed by the diffusion step [41].

The electrolysis of CR (50 ppm, 0.072 mM) with CME was performed with an applied potential of 2.0 V vs. SCE, at room temperature, without hydrogen peroxide. Both clays-modified CME are efficient in degrading the dye by electro-Fenton-like reaction, but Clay<sub>F</sub> is more effective since it removes the dye in less time of reaction than Clay<sub>O</sub>. Fig. 8 shows the results obtained for Clay<sub>F</sub>-modified electrode at the beginning and after

2 h of reaction, as well as the evolution of CR conversion.

The results show that degradation occurs very fast since 81% of the CR molecule is degraded after 5 min, being fully oxidized after 45 min of reaction (Fig. 8). At the end of reaction (2 h), TOC was determined and 67% of mineralization was calculated. A similar value of mineralization (64%) was previously obtained with the best Fe(H)ZSM5-modified electrode [41]. However, on the Clay<sub>F</sub>-modified electrode, CR degradation appears to be faster than on the electrodes modified with Fe-MFI zeolites, on which only 74% of conversion was achieved after 10 min of reaction [41].

HPLC-UV/vis and ionic chromatographic (IC) analyses were employed to quantify the products at the end of reaction. The results reveal the presence of sulfate ions and several low molecular weight carboxylic acids, which are the byproducts of the CR rings opening triggered by the hydroxyl radicals produced during the electro-Fenton reaction (Fig. 9 and Table 4).

The major compounds identified at the end of electrolysis were oxamic, oxalic and adipic acids, and sulfate ions. These recalcitrant products result from the degradation of the dye by the electro-generation of the oxygenated radical species and the presence of Fe(III)-hydroperoxo species. These species come from the oxidation of water in the adopted oxidative conditions since oxygen is produced at

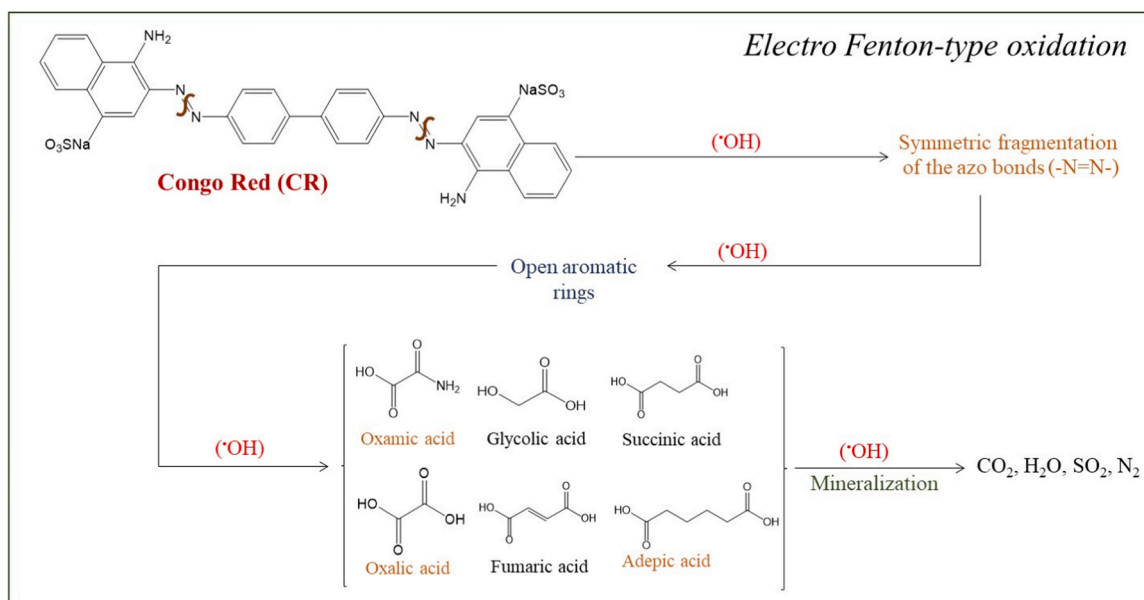


Fig. 10. Proposed mechanism pathway for electro-Fenton reaction of CR.

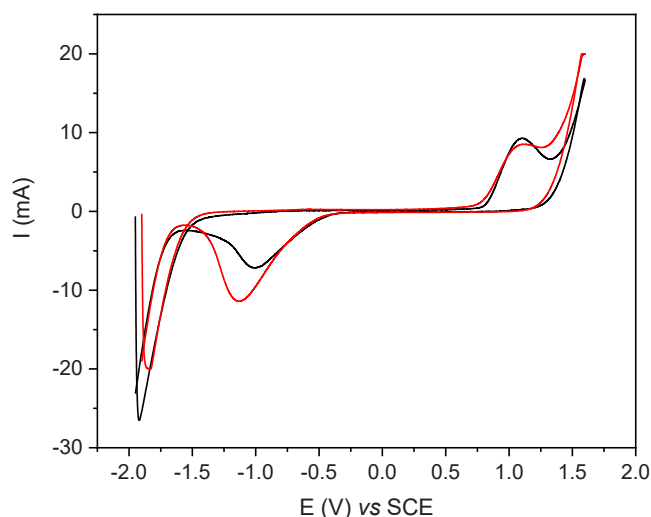


Fig. 11. Cyclic voltammograms of CME based on Clay<sub>F</sub>, recorded at 50 mVs<sup>-1</sup> before (red curve) and after the electrolysis (black curve) of Congo Red dye (0.072 mM) in NaCl (0.10 molL<sup>-1</sup>).

2.0 V vs. SCE [41]. The higher mineralization rate (67%) determined for Clay<sub>F</sub>-CME is probably related to the chemical composition of this raw clay as well as the geological place. As mentioned before, this clay is rich in calcium and has a homogeneous distribution of iron, which enhance the electro-Fenton reaction.

Based on our previous studies [6,26,41] and on the identification of refractory products at the end of electrolysis, CR degradation can occur through the generation of oxygenated radical species, which facilitate the production of small organic acids and sulfate ions, and the successive mineralization of such organic species. The proposed mechanism pathway for CR by the electro-Fenton reaction is presented in Fig. 10.

Fig. 11 shows the cyclic voltammograms recorded before and after the electrolysis in the presence of CME modified with Clay<sub>F</sub>.

The stability of the prepared electrocatalysts was tested by cyclic voltammetry in freshly prepared supporting electrolyte after electrolysis. The shape of the voltammograms remains unchanged after the

electrolysis, which shows that the electrocatalysts have good chemical and mechanical stability. This behavior, which was previously observed also after the CR electrolysis with zeolite-modified electrodes [41], proves the stability of the CLay<sub>F</sub>-based CME.

#### 4. Conclusion

In this study, the Fenton-like reaction was used as the oxidative process for degrading two organic pollutants (Tar and Caf), using three raw clays from Morocco as heterogeneous catalysts. Under the adopted experimental conditions, these clays are more effective in oxidizing tartrazine than caffeine. The best catalytic results were obtained in the presence of Clay<sub>O</sub> and Clay<sub>MA</sub>, with 60.0% and 23.4% of conversion, and 41.0% and 20.5% of mineralization for Tar and Caf, respectively. The introduction of zinc or copper into Clay<sub>MA</sub> does not lead to a significant improvement in the degradation of Tar, the conversion of the metal-containing clay being equal to that of the starting one. However, Cu-Clay<sub>MA</sub> enhances the oxidation of the caffeine molecule (32.4%) compared to the pristine clay. Moreover, the electro-Fenton-like reaction was found to promote the oxidation of CR at room temperature with a high mineralization degree (67%), avoiding the use of redox agents. Our study shows that the raw clays from Morocco can be successfully applied in water treatments as a low-cost heterogeneous catalyst for a sustainable process.

#### CRediT authorship contribution statement

**Ouissal Assila:** Formal analysis, Investigation, Writing – original draft. **Zineb Bencheqroun:** Formal analysis, Methodology, Investigation, Writing – original draft. **Elisabetta Rombi:** Validation, Writing – review & editing. **Teresa Valente:** Writing – review & editing. **Amália S. Braga:** Formal analysis. **Hicham Zaitan:** Validation, Writing – review & editing. **Abdelhak Kherbeche:** Validation, Writing – review & editing. **Olívia S.G.P. Soares:** Investigation, Validation, Writing – review & editing. **Manuel F.R. Pereira:** Validation, Writing – review & editing. **António M. Fonseca:** Methodology, Validation, Writing – review & editing. **Pier Parpot:** Methodology, Validation, Writing – review & editing. **Isabel C. Neves:** Conceptualization, Methodology, Validation, Writing – review & editing, Funding acquisition, Supervision. All authors have read and agreed to the published version of the manuscript.

## Declaration of Competing Interest

All authors declare do not have a Conflict of Interest.

## Data availability

Data will be made available on request.

## Acknowledgments

O.A. and Z.B. thank to ERASMUS+ Program for the mobility PhD grants. This research work has been funded by national funds funded through FCT/MCTES (PIDDAC), (Fundação para Ciência e Tecnologia, FCT) over the projects: LA/P/0045/2020 (ALICE), UIDB/50020/2020 and UIDP/50020/2020 (LSRE-LCM), Centre of Chemistry (UID/UI/0686/2020) and project BioTecNorte (operation NORTE-01-0145-FEDER-000004), supported by the Northern Portugal Regional Operational Programme (NORTE 2020), under the Portugal 2020 Partnership Agreement, through the European Regional Development Fund (ERDF).

## Appendix A. Supporting information

Supplementary data associated with this article can be found in the online version at [doi:10.1016/j.colsurfa.2023.132630](https://doi.org/10.1016/j.colsurfa.2023.132630).

## References

- S. Axon, D. James, The UN Sustainable Development Goals: How can sustainable chemistry contribute? A view from the chemical industry, *Curr. Opin. Green. Sustain. Chem.* 13 (2018) 140–145, <https://doi.org/10.1016/j.cogsc.2018.04.010>.
- United Nations, Sustainable development knowledge platform, sustainable development goals, 2016. (<https://sustainabledevelopment.un.org/sdgs>).
- P.T. Anastas, J.B. Zimmerman, The molecular basis of sustainability, *Chem* 1 (2016) 10–12, <https://doi.org/10.1016/j.chempr.2016.06.016>.
- United Nations, 2023, (<https://www.un.org/sustainabledevelopment/wp-content/uploads/2019/07/UNSG-Roadmap-Financing-the-SDGs-July-2019.pdf>).
- Z. Bencheqroun, I. El Mrabet, M. Kachabi, M. Nawdali, H. Valdés, I. Neves, H. Zaitan, Removal of basic and acid dyes from aqueous solutions using cone powder from Moroccan cypress *Cupressus sempervirens* as a natural adsorbent, *Desalin. Water Treat.* 166 (2019) 387–398, <https://doi.org/10.5004/dwt.2019.24514>.
- O. Assila, Ó. Barros, A.M. Fonseca, P. Parpot, O.S.G.P. Soares, M.F.R. Pereira, F. Zerrouq, A. Kherbeche, E. Rombi, T. Tavares, I.C. Neves, Degradation of pollutants in water by Fenton-like oxidation over LaFe-catalysts: Optimization by experimental design, *Microporous Mesoporous Mater.* 3491 (2023), 112422, <https://doi.org/10.1016/j.micromeso.2022.112422>.
- A. Aid, R.D. Andrei, A. Samira, C. Cammarano, D. Nibou, H. Vasile, Ni-exchanged cationic clays as novel heterogeneous catalysts for selective ethylene oligomerization, *Appl. Clay Sci.* 146 (2017) 432–438.
- H.B. Hadjitaief, M.E. Galvez, M.B. Zina, P. Costa, TiO<sub>2</sub>/clay as a heterogeneous catalyst in photocatalytic/photochemical oxidation of anionic reactive blue 19, *Arab. J. Chem.* 12 (7) (2019) 1454–1462.
- J. Herney-Ramirez, M.A. Vicente, L.M. Madeira, Heterogeneous photo-Fenton oxidation with pillared clay-based catalysts for wastewater treatment: a review, *Appl. Catal. B Environ.* 98 (2010) 10–26.
- J.H.F. Jesus, K.V.L. Lima, R.F.P. Nogueira, Copper-containing magnetite supported on natural clay as a catalyst for heterogeneous photo-Fenton degradation of antibiotics in WWTP effluent, *J. Environ. Chem. Eng.* 10 (3) (2022), 107765.
- R. Antonelli, G.R.P. Malpass, M.G.C. da Silva, M.G.A. Vieira, Adsorption of ciprofloxacin onto thermally modified bentonite clay: experimental design, characterization, and adsorbent regeneration, *J. Environ. Chem. Eng.* 8 (2020), 104553.
- G.G. Haciosmanoglu, C. Mejias, J. Martín, J.L. Santos, I. Aparicio, E. Alonso, Antibiotic adsorption by natural and modified clay minerals as designer adsorbents for wastewater treatment: A comprehensive review, *J. Environ. Manag.* 317 (2022), 115397.
- A.S. Maryan, M. Montazer, R. Damerchely, Discoloration of denim garment with color free effluent using montmorillonite based nano clay and enzymes: nano bio-treatment on denim garment, *J. Cleaner Production* 91 (2015) 208–215.
- R.A. Schoonheydt, Clays: from two to three dimensions, in *Introduction to zeolite science and practice*, in: H. van Bekkum, E.M. Flanigen, J.C. Jansen (Eds.), *Studies in Surface Science and Catalysis*, V. 58, Elsevier, Netherlands, 1991, pp. 201–239.
- H. Fida, G. Zhang, S. Guo, A. Naeem, Heterogeneous Fenton degradation of organic dyes in batch and fixed bed using La-Fe montmorillonite as catalyst, *J. Colloid Interface Sci.* 490 (2017) 859–868, <https://doi.org/10.1016/j.jcis.2016.11.085>.
- W. Fu, J. Yi, M. Cheng, Y. Liu, G. Zhang, L. Li, L. Du, B. Li, G. Wang, X. Yang, When bimetallic oxides and their complexes meet Fenton-like process, *J. Hazard. Mater.* 424 (2022), 127419, <https://doi.org/10.1016/j.jhazmat.2021.127419>.
- Y. Liu, Y. Zhao, J. Wang, Fenton/Fenton-like processes with in-situ production of hydrogen peroxide/hydroxyl radical for degradation of emerging contaminants: Advances and prospects (doi.org/), *J. Hazard. Mater.* 404 (2021), 124191, <https://doi.org/10.1016/j.jhazmat.2020.124191>.
- M. Usman, O. Monfort, S. Gowrisankaran, B.H. Hameed, K. Hanna, M. Al-Abri, Dual functional materials capable of integrating adsorption and Fenton-based oxidation processes for highly efficient removal of pharmaceutical contaminants, *J. Water Process Eng.* 52 (2023), 103566, <https://doi.org/10.1016/j.jwpe.2023.103566>.
- J. Wang, J. Tang, Fe-based Fenton-like catalysts for water treatment: Preparation, characterization and modification, *Chemosphere* 276 (2021), 130177, <https://doi.org/10.1016/j.chemosphere.2021.130177>.
- E. Brillas, I. Sires, M.A. Oturan, Electro-Fenton process and related electrochemical technologies based on Fenton's reaction chemistry, *Chem. Rev.* 109 (2009) 6570–6631.
- B.P. Chaplin, Critical review of electrochemical advanced oxidation processes for water treatment applications, *Environ. Sci. Process. Impacts* 16 (2014) 1182–1203.
- V. Poza-Nogueiras, E. Rosales, M. Pazos, M.A. Sanrom, Current advances and trends in electro-Fenton process using heterogeneous catalysts: A review, *Chemosphere* 201 (2018) 399–416.
- A. Ozcan, A.A. Ozcan, Y. Demirci, E. Sener, Preparation of Fe<sub>2</sub>O<sub>3</sub> modified kaolin and application in heterogeneous electro-catalytic oxidation of enoxacin, *Appl. Catal. B Environ.* 200 (2017) 361–371.
- H. Ma, Q. Zhuo, B. Wang, Electro-catalytic degradation of methylene blue wastewater assisted by Fe<sub>2</sub>O<sub>3</sub>-modified kaolin, *Chem. Eng. J.* 155 (2009) 248e253.
- E.G. Garrido-Ramírez, M.L. Mora, J.F. Marco, M.S. Ureta-Zanartu, Characterization of nanostructured allophane clays and their use as support of iron species in a heterogeneous electro-Fenton system, *Appl. Clay Sci.* 86 (2013) 153–161.
- O. Assila, N. Vilaça, A.R. Bertão, A.M. Fonseca, P. Parpot, O.S.G.P. Soares, M.F. R. Pereira, F. Baltazar, M. Bañobre-López, I.C. Neves, Optimization of iron-ZIF-8 catalysts for degradation of tartrazine in water by Fenton-like reaction, *Chemosphere* 339 (2023), 139634, <https://doi.org/10.1016/j.chemosphere.2023.139634>.
- M. Ferreira, I.K. Biernacka, A.M. Fonseca, I.C. Neves, O.S.G.P. Soares, M.F. R. Pereira, J.L. Figueiredo, P. Parpot, Study of the Electroreactivity of Amoxicillin on Carbon Nanotube-Supported Metal Electrodes, *ChemCatChem* 10 (2018) 4900–4909.
- F. Bergaya, The meaning of surface area and porosity measurements of clays and pillared clays, *J. Porous Mater.* 2 (1995) 91–96.
- J.T. Klopogge, Synthesis of smectites and porous pillared clay catalysts: a review, *J. Porous Mater.* 5 (1998) 5–41.
- P.G. Weidler, BET sample pretreatment of synthetic ferrihydrite and its influence on the determination of surface area and porosity, *J. Porous Mater.* 4 (1997) 165–169.
- J.Q. Jiang, S.M. Ashekuzzaman, J.S.J. Hargreaves, A.R. Mcfarlane, A.B. M. Badruzaman, M.H. Tarek, Removal of arsenic (III) from groundwater applying a reusable Mg-Fe-Cl layered double hydroxide, *J. Chem. Technol. Biotechnol.* 90 (2015) 1160–1166.
- D.M. Moore, R.C. Reynolds, *X-ray Diffraction and Identification and Analysis of Clay Minerals*, 2nd edition, Oxford University Press, New York, 1997.
- C. Elmi, S. Guggenheim, R. Gieré, Surface crystal chemistry of phyllosilicates using X-ray photoelectron spectroscopy: a review, *Clay Clay Min* 64 (5) (2016) 537–551.
- Handbook of X-ray Photoelectron Spectroscopy, A reference book of standard spectra for identification and interpretation of XPS data, in: Jill Chastain (Ed.), Physical Electronics Division, Perkin-Elmer Corporation, 1992.
- A.V. Naumkin, A. Kraut-Vass, S.W. Gaarenstroom, C.J. Powell, N.I.S.T. X-ray Photoelectron Spectroscopy Database, NIST Standard Reference Database 20, Version 4.1, Last Update to Data Content: 2012, (<https://doi.org/10.18434/T4T88K>).
- G.O. Ihekwe, J.N. Shondo, K.I. Orisekeh, G.M. Kalu-Uka, I.C. Nwuzor, A. P. Onwualu, Characterization of certain Nigerian clay minerals for water purification and other industrial applications, *Heliyon* 6 (2020) 03783.
- M. Todea, E. Vanea, S. Bran, P. Berce, S. Simon, XPS analysis of aluminosilicate microspheres bioactivity tested in vitro, *Appl. Surf. Sci.* 270 (2013) 777–783.
- H. Tissot, L. Li, S. Shaikhutdinov, H.J. Freund, Preparation and structure of Fe containing aluminosilicate thin films, *Phys. Chem. Chem. Phys.* 18 (36) (2016) 25027–25035.
- A.D. Bokare, W. Choi, Review of Iron-free Fenton-like Systems for Activating H<sub>2</sub>O<sub>2</sub> in Advanced Oxidation Processes, *J. Hazard. Mater.* 275 (2014) 121–135.
- B.L.C. Santos, P. Parpot, O.S.G.P. Soares, M.F.R. Pereira, E. Rombi, A.M. Fonseca, I. C. Neves, Fenton-Like Bimetallic Catalysts for Degradation of Dyes in Aqueous Solutions, *Catalysts* 11 (2021) 32, <https://doi.org/10.3390/catal11010032>.
- Z. Bencheqroun, N.E. Sahin, O.S.G.P. Soares, M.F.R. Pereira, H. Zaitan, M. Nawdali, E. Rombi, A.M. Fonseca, P. Parpot, I.C. Neves, Fe(III)-exchanged zeolites as efficient electrocatalysts for Fenton-like oxidation of dyes in aqueous phase, *J. Environ. Chem. Eng.* 10 (2022), 107891, <https://doi.org/10.1016/j.jece.2022.107891>.